Nimbus-5 ESMR Polar Gridded Sea Ice Concentrations, Version 1

USER GUIDE

How to Cite These Data

As a condition of using these data, you must include a citation:

Parkinson, C. L., J. C. Comiso, and H. J. Zwally. Edited by W. N. Meier and J. Stroeve. 2004. *Nimbus-5 ESMR Polar Gridded Sea Ice Concentrations, Version 1.* [Indicate subset used]. Boulder, Colorado USA. NASA National Snow and Ice Data Center Distributed Active Archive Center. https://doi.org/10.5067/W2PKTWMTY0TP. [Date Accessed].

FOR QUESTIONS ABOUT THESE DATA, CONTACT NSIDC@NSIDC.ORG

FOR CURRENT INFORMATION, VISIT https://nsidc.org/data/NSIDC-0009

National Snow and Ice Data Center

TABLE OF CONTENTS

1 DATA DESCRIPTION

The Nimbus-5 Electrically Scanning Microwave Radiometer (ESMR) data set provides the earliest all-weather, all-season imagery of polar sea ice. Daily and monthly averaged sea ice concentrations from the ESMR are available for the Arctic and Antarctic. Some satellite data of sea ice in the visible and infrared wavelengths were available in the late 1960s and early 1970s, but since the polar regions are either dark or cloud-covered for much of the year, the generation of consistent, long-term data records from visible and infrared sensing was not practical.

The passive microwave data collected by the Nimbus-5 ESMR introduced a major advance in the usefulness of satellite sea ice imaging. The value of the ESMR data for sea ice studies derives from the large contrast in microwave emissivities between sea ice and open water. At the 19 GHz frequency of the ESMR, open water has an emissivity of approximately 0.44, whereas various sea ice types have emissivities ranging from approximately 0.8 to 0.97. The resulting contrast in microwave brightness temperatures allow conversions to approximate sea ice concentrations (percentages of ocean area covered by sea ice) and hence identification of sea ice distributions throughout the region of observation, as well as temporal variations of these distributions throughout the time period of observation.

1.1 Format

Data are in HDF format. The size of the arrays are 304 columns x 448 rows for the Arctic and 316 columns x 332 rows for the Antarctic. Pixel values for ice concentration range from 0 to 100 (0-100 percent ice concentration). Flag values for land and missing pixels are consistent with other NSIDC SSM/I ice concentration products; however, additional flags are included for ESMR:

Missing = 157
Land = 168
Coast = 178
Ocean = 125 (from the ocean mask)
Lakes = 120
Low ice concentration = 200-215 (corresponding to concentration values of 0-15%)

1.2 Directory Structure

Data are available on the HTTPS site in the https://daacdata.apps.nsidc.org/pub/DATASETS/nsidc0009_esmr_seaice/ directory. Within this directory there are two folders, north and south. Refer to Table 1 for a listing of the files within the north and south folders.

Table 1. HTTPS Directory Folder Description

Folders	Descriptions
bad	Data with bad scans and other errors that were not used in the monthly averages or climatological means. See Processing Steps in this document for a list of dates for which data were removed.
daily00	Daily fields with ice concentration threshold of 0%
daily15	Daily fields with ice concentration threshold of 15%
means	Climatological means for each month, 1973-1976
monthly	Monthly averages and files that list the number of samples at each pixel location

1.3 File Naming Convention

This section explains the file naming convention used for this product with examples. Table 2 lists example file names and the variables used in the file names.

Table 2. Example File Names and Variables

Folder Name	Example North Folder File Names	Example South Folder File Names	Variables Used in the File Name
bad	ESMR-1973023.tne.15	ESMR-1973062.tse.15	ESMR-1973023.xxx.15
daily00	ESMR-1972346.tne.00.gz	ESMR-1972346.tse.00.gz	ESMR-yyyyddd.xxx.00.gz
daily15	ESMR-1972346.tne.15.gz	ESMR-1972346.tse.15.gz	ESMR-yyyyddd.xxx.15.gz
means	ESMR-1973-1976-01.tne.15.gz	ESMR-1973-1976-01.tse.15.gz	ESMR-1973-1976-mm.xxx.15.gz
monthly	ESMR-197212.count.tne.15.gz ESMR-197212.tne.15.gz	ESMR-197212.count.tse.15.gz ESMR-197212.tse.15.gz	ESMR-yyyymm.count.xxx.15.gz (Files containing the number of samples at each pixel in the monthly mean field) ESMR-yyyymm.xxx.15.gz

Refer to Table 3 for the values for the file name variables listed above.

Table 3. Values for File Name Variables

Variable	Description
yyyy	4-digit year
mm	2-digit month
ddd	3-digit day of year

Variable	Description
xxx	t = total ice concentration n = Northern hemisphere s = Southern hemisphere e = ESMR single-channel algorithm
00	0% ice concentration threshold
15	15% ice concentration threshold
.gz	compressed file

1.4 File Size

Arctic files are 138 KB, and Antarctic files are 107 KB.

1.5 Usage

Users wishing to create custom sea ice concentrations should refer to the Appendix for information on calculating ice concentration from brightness temperatures. Please note, however, that it may be difficult to compare these sea ice concentrations with the SMMR and SSM/I sea ice concentrations, because no overlap period exists between the SMMR and ESMR instruments. Additionally, because ESMR has just one channel of data, the sea ice concentrations derived from ESMR may not be as accurate as those derived from the SMMR and SSM/I instruments.

1.6 Spatial and Temporal Information

1.6.1 Spatial Coverage

Instrument coverage is global except for circular sectors centered over the poles, 280 km in radius, poleward of 87°N and 87°S, which are never measured due to orbit inclination. Data set coverage includes the polar regions defined by the spatial coverage map below.

1.6.2 Spatial Coverage Map

ESMR data are gridded to a polar stereographic projection with the following coverage:

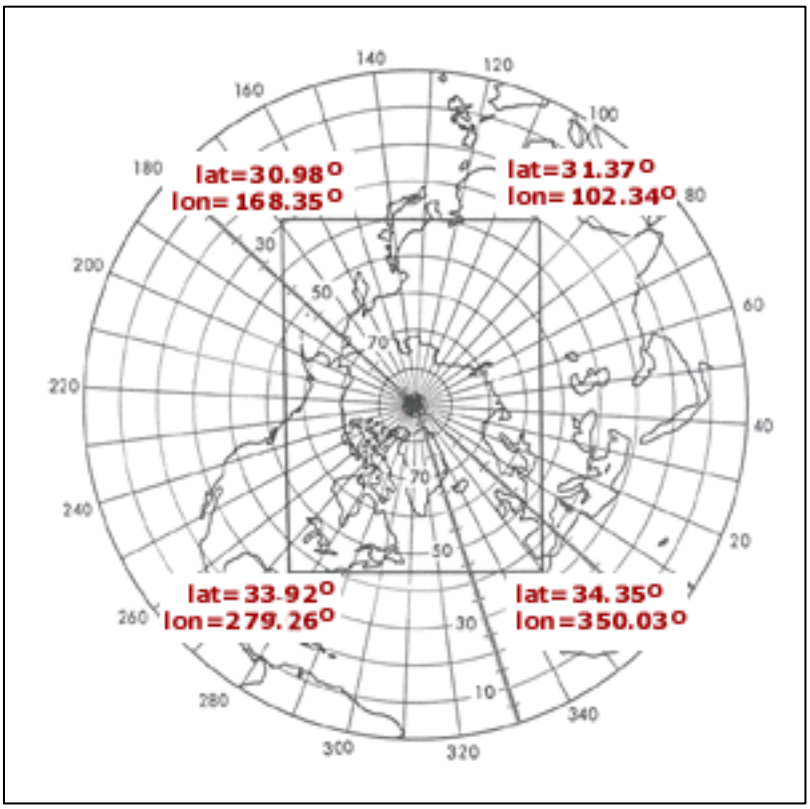

Figure 1. Northern Hemisphere

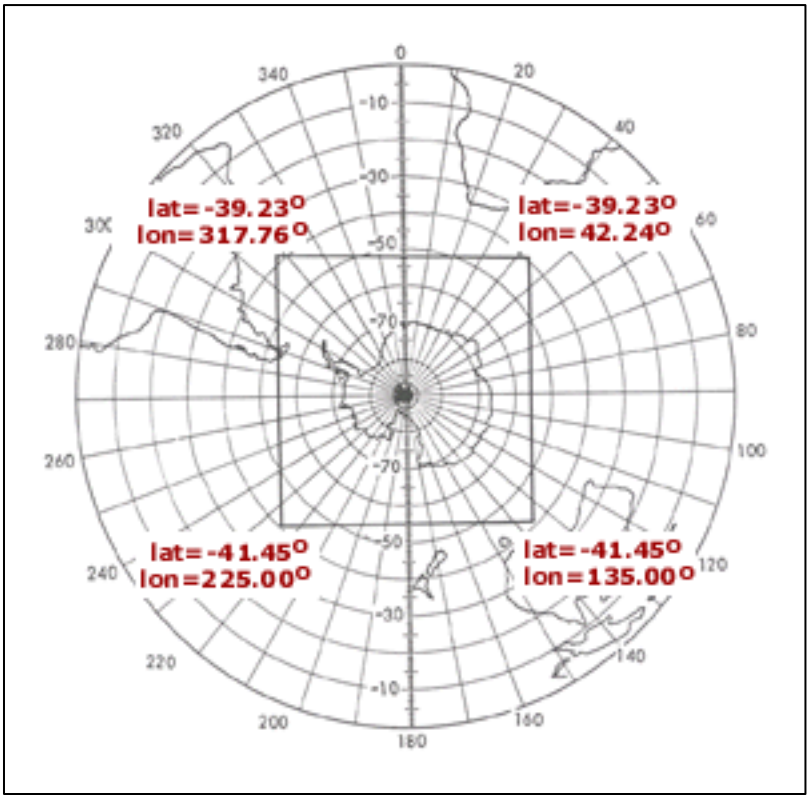

Figure 2. Southern Hemisphere

1.6.3 Spatial Resolution

The ESMR footprint size varies from approximately 32 km x 32 km to about 28 km x 28 km at 50° latitude. Gridded resolution is 25 km.

1.6.4 Projection

ESMR sea ice grids are in a polar stereographic projection, which specifies a projection plane, such as the grid, tangent to the earth at 70 degrees. The planar grid is designed so that the grid cells at 70 degrees latitude are 25 km x 25 km. Refer to Pearson (1990) and Snyder (1987) for more information on this topic.

The polar stereographic projection often assumes that the plane (grid) is tangent to the Earth at the pole. Thus, there is a one-to-one mapping between the Earth's surface and grid (with no distortion) at the pole. Distortion in the grid increases as the latitude decreases because more of the Earth's surface falls into any given grid cell, which can be quite significant at the edge of the northern polar grid where distortion reaches 31 percent. The southern polar grid has a maximum distortion of 22 percent. To minimize the distortion, the projection is true at 70 degrees rather than at the poles. This increases the distortion at the poles by three percent and decreases the distortion at the grid boundaries by the same amount. The latitude of 70 degrees was selected so that little or no distortion would occur in the marginal ice zone. Another result of this assumption is that fewer grid cells are required as the Earth's surface is more accurately represented.

The polar stereographic formulae for converting between latitude/longitude and X-Y grid coordinates are taken from Snyder (1982). This projection assumes a Hughes ellipsoid with a radius of 3443.992 nautical mi or 6378.273 km and an eccentricity (e) of 0.081816153 (or e**2 = 0.006693883).

1.6.5 Grid Description

North: 304 columns, 448 rows
South: 316 columns, 332 rows

Polar Stereographic Grid Coordinates

The origin of each x, y grid is the pole. The grids' approximate outer boundaries are defined in the following table. Corner points are listed; apply values to the polar grids reading clockwise from upper left. Interim rows define boundary midpoints.

Table 4. North Polar

X (km)	Y (km)	Latitude (deg)	Longitude (deg)	
-3850	5850	30.98	168.35	corner
0	5850	39.43	135.00	midpoint
3750	5850	31.37	102.34	corner
3750	0	56.35	45.00	midpoint
3750	-5350	34.35	350.03	corner
0	-5350	43.28	315.00	midpoint
-3850	-5350	33.92	279.26	corner
-3850	0	55.50	225.00	midpoint

Table 5. South Polar

X (km)	Y (km)	Latitude (deg)	Longitude (deg)	
-3950	4350	-39.23	317.76	corner
0	4350	-51.32	0.00	midpoint
3950	4350	-39.23	42.24	corner
3950	0	-54.66	90.00	midpoint
3950	-3950	-41.45	135.00	corner
0	-3950	-54.66	180.00	midpoint
-3950	-3950	-41.45	225.00	corner
-3950	0	-54.66	270.00	midpoint

1.6.6 Temporal Coverage

The temporal coverage for this data set ranges from 13 December 1972 through 11 May 1977. However, these dates vary depending on the file type. Refer to Table 6 for a listing of the temporal coverage dates for each file type.

Table 6. Temporal Coverage Dates by File Type

File Type	Dates
Monthly Files	13 December 1972 to March 1977
Mean Files	January 1971 to December 1976
00% and 15% Daily Files	13 December 1973 to 11 May 1977

Tables 7 and 8 list the dates of bad data for both hemispheres.

Table 7. Bad Data for the Northern Hemisphere

Year	Day of Year
1972	346
1973	23, 29, 38, 44, 150
1974	31, 66, 310, 315, 359, 362
1975	28, 288, 300-302
1976	40, 98
1977	131

Table 8. Bad Data for the Southern Hemisphere

Year	Day of Year
1973	63-147, 217-241, 266, 280, 284, 287, 297, 334, 335
1974	13-15, 84-95, 129, 136, 184, 212-220, 252, 295-298, 305
1975	62, 76, 91-97, 106, 108-115, 117, 150
1976	217, 272, 314, 334, 346
1977	72, 88-100

1.6.7 Temporal Resolution

Daily and monthly averaged data are provided.

1.7 Parameter or Variable

1.7.1 Parameter Description

Sea ice concentration is the fraction of a given area covered by sea ice irrespective of ice type, or the ratio describing the areal density of ice in a given area.

1.7.2 Unit of Measurement

Ice concentration values are given as percentages.

1.7.3 Parameter Source

These data are derived from Nimbus-5 ESMR brightness temperatures, originally processed by the Goddard Space Flight Center (GSFC). NSIDC obtained the data from GSFC and reproccesed them to remove coastal and weather contamination, and to include a 15 percent ice threshold.

1.7.4 Parameter Range

Pixel values range from 0 to 255.

1.7.5 Error Sources

The Processing Steps section of this document discusses removal of some errors from the original data.

1.7.6 Quality Assessment

The Processing Steps section of this document discusses quality control steps taken.

2 SOFTWARE AND TOOLS

Because ESMR brightness temperatures are in the same polar stereographic grid as SSM/I brightness temperatures, some SSM/I tools can be used to read and display the ESMR data. Included are IDL display programs to extract and display the data, geolocation (geocoordinate) tools, and pixel-area grids. Table 9 lists the tools that can be used with this data set. For a comprehensive list of all polar stereographic tools and for more information, see the Polar Stereographic Data Tools Web page.

Table 9. Tools for this Data Set

Tool Type	Tool File Name(s)
Data Extraction	`extract_ice.pro`
Geocoordinate	`locate.for`
	`mapll.for and mapxy.for`
	`psn25lats_v3.dat and pss25lats_v3.dat`
	`psn25lons_v3.dat and pss25lons_v3.dat`
Pixel-Area	`psn25area_v3.dat and pss25area_v3.dat`

3 DATA ACQUISITION AND PROCESSING

3.1 Theory of Measurements

Refer to the Appendix of this document for calculations of sea ice concentration from brightness temperatures.

3.2 Data Acquisition Methods

Telemetry data from the Nimbus-5 satellite were transmitted to two spaceflight tracking and data network stations located near Fairbanks, Alaska, and Rosman, North Carolina. The data were relayed from these stations to the NASA Goddard Space Flight Center (GSFC). At GSFC, the telemetry data were unpacked, decommutated, supplemented with flags and ends of files, and stored on magnetic tapes called experimental tapes (ETs). For data processing convenience, the data from the ESMR instrument were combined from several ETs to form stacked experimental tapes (SETs). The 10-bit telemetry data on the ETs were converted to 32-bit format on the SETs for use on the GSFC computers. The SETs were used with ephemeris tapes to generate Earth-located calibrated brightness temperature (CBT) tapes.

3.3 Derivation Techniques and Algorithms

3.3.1 Calculating Sea Ice Concentration from ESMR

Variations in the brightness temperature (T_b) observed over the surface of the Earth are caused by variations in the emissivity of the surface material and variations in physical temperature according to the equation:

$$\mathbf{T_b = \varepsilon_T} \qquad [1]$$

This equation is valid for the brightness temperatures of a uniform surface type with emissivit ε and physical temperature T. Within the ice pack, the brightness temperatures of a pixel area derives from various sources, including atmospheric contributors as well as the water and ice within the field of view. The brightness temperatures of ice with uniform emissivity is approximated as:

$$\mathbf{T_b = C_W \varepsilon_W T_W + C_I \varepsilon_I T_I + T_A} \qquad [2]$$

Where:

ε_W = Emissivity of open water
T_W = Surface physical temperature of open water
C_W = Areal percentage of open water
ε_I = Emissivity of sea ice
T_I = Surface physical temperature of sea ice
C_I= Areal percentage of sea ice
T_A= Sum of atmospheric and other above-surface contributions, including direct upwelling radiation from the atmosphere, downwelling radiation reflected by the surface, and radiation from space reflected by the surface. Atmospheric opacity in the polar regions is negligible.

Recognizing that $C_W + C_I = 1$, the ice concentration C_I, can be determined from Equation [2] as:

$$\mathbf{C_I = T_b - T_0 / \varepsilon_I T_{eff} - T_0} \qquad [3]$$

Where:

$T_0 = \varepsilon_W T_W + T_A$, the measured T_b of the water
$T_{eff} = T_I\& + T_A / \varepsilon_I$, the effective surface physical temperature.

In the polar regions, the atmospheric contribution to the effective temperature is small because the atmospheric humidity and the water vapor content are very low; therefore, T_{eff} is equal to T_I. The appropriate value for T_I is the temperature at the top of the sea ice below the snow cover, because most of the observed radiation emanates from a thin top layer of saline ice. In the absence of real-time physical temperature data, T_I is estimated from climatological surface air temperatures in Equation [4] below. The temperature at the top surface of the sea ice is calculated as lying between the surface air temperature T_{air} -- estimated by mean monthly climatological values -- and the temperature of the water underneath the ice:

$$\mathbf{T_I = T_{air} + f(T_f - T_{air})} \qquad [4]$$

Where:

T_f = Freezing point of sea water, 271.2 K

f = Empirical parameter determined from the observed brightness temperatures data, by adjusting f until the values of C_I are consistently about 100% during winter. A value of f = 0.25 was used in the Antarctic atlas (Zwally et al. 1983) through examination of the July 1974 data over the Southern Ocean. Later examination of the Northern Hemisphere data showed that f = 0.25 is also appropriate for the Arctic. This value of 0.25 agrees with the overall average of surface measurements made at Pond Inlet in the Canadian Archipelago (R. Ramseier, personal communication). In reality, the magnitude of f varies spatially with the thickness of the ice and snow cover, but f = 0.25 appears to be a reasonable average value.

Analysis of brightness temperatures from the open-ocean area in the vicinity of the ice pack allowed determination of T_0 for use in Equation [1]. Specifically, the four-year average of brightness temperatures over ice-free areas of the north polar region was calculated from the ESMR observations as 138.3 K. This is the value inserted for T_0. Of the 138.3 K, approximately 120 K derives from the water, and the remainder derives from the atmosphere. In the Antarctic, the similarly calculated T_0 is 135 K. The 3.3 K difference between hemispheres is caused predominantly by actual differences in the average signature of ice-free ocean in the two hemispheres. It could also be caused in part by variations in the sensitivity of the instrument with

temperature. The satellite is exposed to solar heating as it approaches the north polar region but not in the south polar region.

The ice concentration parameter is generated from Equation [2] using T_0 = 138.3 K, T_{eff} = T_I (calculated from Equation [3]), and ε_I = 0.92. The emissivity value of 0.92 is estimated from radiative equations appropriate for first-year sea ice, and is confirmed empirically for first-year ice by examination of ESMR data; however, many regions of the Arctic contain significant amounts of multiyear ice, which has an emissivity of approximately 0.84 instead of 0.92; hence, the gridded data can be interpreted directly as ice concentrations only in those grid squares containing open water and first-year sea ice; otherwise, the data should be interpreted using a nomogram in which both ice concentration, C, and multiyear ice fraction, F_{MY} are represented as variables. The crucial element in the generation of the nomogram is the proper placement of the concentration values on the right-hand scale, corresponding to a field of view with exclusively multiyear ice and open water. The right-hand scale on the nomogram was constructed by recognizing that the concentrations C_I calculated with a first-year ice emissivity were determined by:

$$\mathbf{C_1 = T_b - T_0 / 0.92T_I - T_0} \qquad [5]$$

Where T_0= 183.3 K.

For multiyear ice, the equation is:

$$\mathbf{C_{MY} = T_b - T_0 / 0.84T_I - T_0 = C_I[(0.92T_I - T_0) / (0.84T_I - T_0)]} \qquad [6]$$

Inserting 248 K as an appropriate overall value for T_I, Equation [6] reduces to C_{MY} = 1.283 C_I, which is the conversion used in creating the nomogram. In the Arctic atlas, the ice concentration maps and nomograms are color-coded, with, for instance, the boundary between light pink and deep brown occurring at 78 percent concentration for first-year ice. During periods of surface melting, first-year and multiyear ice are indistinguishable by passive microwave measurements (Parkinson et al. 1987), and the appropriate scale for both ice types is the scale on the left of the nomogram.

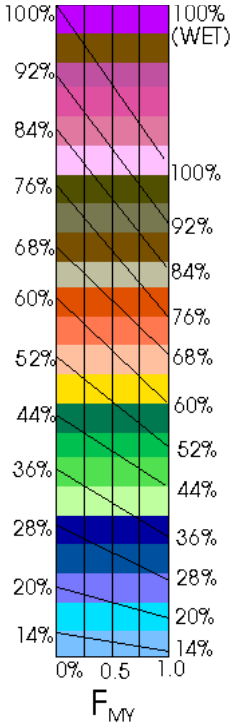

Figure 3. Ice Concentration Nomogram

Differences between wet and dry first-year ice, which are about 3 percent, are neglected in the nomogram. The values on tape are termed "pseudo ice concentrations."

This nomogram should be used to interpret pseudo ice concentrations gridded on the magnetic tapes. A given gridded value is associated with a unique ice concentration only if the multiyear ice fraction F_{MY} is known. For instance, in seasonal sea ice regions with only first-year ice, $F_{MY} = 0$. The appropriate scale is shown on the left of the nomogram, so that the gridded values are indeed the calculated ice concentrations. By contrast, in locations where the observed ice field is all multiyear ice ($F_{MY} = 1$), then the appropriate scale is on the right-hand side of the nomogram, and the ice concentrations are derived by multiplying the gridded values by 1.283. If no information is known about the multiyear ice fraction, then the nomoram provides the appropriate range of ice concentrations for each gridded value, with the range extending from the gridded value on the left-hand scale to the value horizontally opposite it on the right-hand scale. For instance, a gridded value of 52 percent indicates an ice concentration anywhere from 52 percent (if there is no multiyear ice) to 67 percent (if the ice is all multiyear ice). The nomogram can also be used in an inverted manner to determine the multiyear ice fraction, if there is independent knowledge (or an estimate) of the total ice concentration. This method was done for the Arctic atlas in several cases where the total ice concentration approaches 100 percent.

3.3.2 Processing Steps

GSFC regridded the original ESMR data to a polar stereographic projection. Data gaps in the original data were filled in using a temporal average of the day before and day after, over the entire field. These data do not include ocean masks and weather filters, and days with bad scans still remain. In Autumn 2003, NSIDC reprocessed these data with the following steps:

1. An ocean mask was applied to remove most weather effects and coastal contamination. Refer to the Monthly Ocean Masks and Maximum Extent Masks Web page for more information. The masks are created from SMMR and SSM/I Bootstrap sea ice concentrations. Climatological masks for each month are produced from the length of the time series, November 1978 through September 2002. Any pixel that did not include ice during the time series is classified as ocean. An additional buffer of two pixels (~50 km) is added to the ice edge to make the mask more conservative; thus, the mask is unlikely to mask out legitimate ice retrievals in the ESMR fields. But weather effects in the remaining open water regions, between the ESMR ice edge and the ocean pixels in the mask, are not removed.

2. To remove some of the remaining weather effects, fields with a 15 percent threshold of ice concentration are included. Thus, any pixel with less than 15 percent ice is considered ice-free. A value of 200 is added to low ice concentrations (0-15%); thus, values of 200-215 indicate low ice concentration. Low ice concentrations can be recovered by simply subtracting 200 from values greater than or equal to 200. Using 15 percent to define the ice edge is consistent with previous studies showing that the 15 percent isopleth in passive microwave ice concentrations corresponds best with the true ice edge. However, some low ice concentrations may be eliminated with this method. In addition, some weather effects leading to false concentrations greater than 15 percent are not removed.

3. Remaining ice concentration errors from bad scans were removed. Errors ranged from a few scan lines to entire fields with bad data, the latter occurring primarily in the Southern Hemisphere. These fields are saved in the bad directory for each hemisphere, on the FTP site. Following is a list of dates for which bad data were removed:

   Northern Hemisphere:
   1972: Day 346
   1973: Days 23, 29, 38, 44, 150
   1974: Days 31, 66, 310, 315, 359, 362
   1975: Days 28, 288, 300-302
   1976: Days 40, 98
   1977: Day 131

Southern Hemisphere:

1973: Days 63-147, 217-241, 266, 280, 284, 287, 297, 334, 335

1974: Days 13-15, 84-95, 129, 136, 184, 212-220, 252, 295-298, 305

1975: Days 62, 76, 91-97, 106, 108-115, 117, 150

1976: Days 217, 272, 314, 334, 346

1977: Days 72, 88-100

4. Monthly means were created where sufficient data were available, such as a minimum of 10 samples for a given pixel over an entire month. A disadvantage of this approach, however, is that a small number of samples may not represent the true monthly mean ice conditions. To assist users in judging ice conditions, files containing the number of samples at each pixel in the monthly field are included in the monthly directory on the FTP site.

   Low ice concentration values in the daily fields were included in the monthly means. After computing the monthly means, ice concentration values below 15 percent were set to 0. The flag values are the same as those for daily grids (see Format above), except without an ocean mask; ocean pixels have a 0 percent concentration. Several months during the ESMR time series did not have sufficient data to create a monthly mean. Table 10 indicates which means were produced for each hemisphere (N and S):

Table 10. Means Produced for Each Hemisphere North

Months	Years					
	1972	1973	1974	1975	1976	1977
January		N,S	N,S	N,S	N,S	S
February		N,S	N,S	N,S	N,S	S
March			N,S	N,S	N,S	N,S
April			N,S		N,S	
May			N,S	N,S	N,S	
June		N,S	N,S		N,S	
July		N,S	N,S		N,S	
August			N,S		N,S	
September		N,S	N,S	N,S	N,S	
October		N,S	N,S	N,S	N,S	
November		N,S	N,S	N,S	S	
December	N,S	N,S	N,S	N,S	S	

From January 1973 through December 1976, where ESMR provided coverage throughout the year, a climatology was produced for each month by averaging all available years of monthly means for that month. Up to four fields are averaged for each month, one for each year; however, some monthly mean fields were not created due to insufficient data. In these cases, the climatology may be based on more than four years. The flag values in the fields are the same as in the `monthly` means. These fields are also in the monthly subdirectories within the `north` and `south` directories.

4 SENSOR OR INSTRUMENT DESCRIPTION

ESMR consisted of four major components:

- A phased array microwave antenna consisting of 103 waveguide elements each having its associated electrical phase shifter. The aperture area is 83.3 cm X 85.5 cm. The polarization is linear, parallel to the spacecraft velocity vector.
- A beam steering computer that determines the coil current for each of the phase shifters for each beam position.
- A microwave receiver with a center frequency of 19.35 GHz and an IF bandpass of from 5 to 125 MHz; thus it is sensitive to radiation from 19.225 to 19.475 GHz, except for a 10 MHz gap in the center of the band.
- Timing, control and power circuits.

4.1 Principles of Operation

Unlike conical scan instruments such as the SMMR and SSM/I, the ESMR was a cross-scan instrument, with a resolution of approximately 30 km, which measured primarily the intensity of electromagnetic radiation thermally emitted from the Earth's surface at a wavelength of 1.55 cm (19.35 GHz). The instrument recorded radiation from 78 scan positions, and all observations were first converted to equivalent nadir observations.

4.2 Sensor/Instrument Measurement Geometry

The Nimbus-5 ESMR recorded radiation from 78 scan positions varying ± 50° from the satellite track every four seconds (Wilheit 1972). The beam width is 1.4° x 1.4° near nadir and degrades to 2.2° crosstrack by 1.4° downtrack at the 50° extremes. For a nominal orbit of 1100 km altitude, the resolution is 25 km x 25 km near nadir, degrading to 160 km crosstrack by 45 km downtrack at the ends of the scan. Full coverage of the entire polar area could be obtained from a sequence of six satellite orbits, or one-half day of good data, if all 78 beam positions were used; however, because of the large disparity in the radiometer field of view from the outer beam position to the middle beam position (70 km x 140 km compared with 25 km x 25 km), only the middle 52 beam positions were used for a swath-angle coverage of ± 30.5° and a minimum resolution of 29 km by 42 km. This swath angle corresponds to a spatial coverage of about 1280 km on the Earth's surface.

4.3 Calibration

The radiometer was originally calibrated using hot and cold reference sources. A sky horn measuring the 3 K cosmic background provided the cold-load temperature reference (T_C). The hot-load temperature was provided by reference to a floating ambient termination in the spacecraft. Calibration parameters were gathered from eight scans of data. Calibration temperatures (T_C and T_H) were calculated from multiplex data, and values of four ambient and four cold calibration voltages averaged through the set of eight scans. For each beam position the brightness temperature (T_{in}) corresponding to voltage (V) was then calculated by:

$$T_{IN} = T_H + [(T_C - T_H)/(V_C - V_H)] (V - V_H)$$

Refer to the “Additional Calibration” section in the Nimbus-5 ESMR Daily Polar Gridded Brightness Temperatures data set documentation for information about further adjustment in the source brightness temperature.

The Nimbus-5 flew in a circular sun-synchronous orbit at 1112 km (600 nautical miles), had a local noon (ascending) and midnight (descending) equator crossing, and an 81 degree retrograde inclination. Successive orbits crossed the equator at 27 degree longitude separation. The orbital period was about 107 minutes. Nimbus-5 used an attitude control system which stabilized the spacecraft with respect to the earth and orbital plane, such that the yaw axis pointed normal to the earth and the roll axis aligned with the spacecraft velocity vector, and which also maintained the solar paddles' orientation to the sun. The system permitted fine control of ± 1° in pitch and ± 0.5° in roll and yaw.

4.4 Source or Platform Mission Objectives

The Nimbus-5 mission had two major goals:

1. To help meet the objectives of NASA's expanding meteorological program (in 1972, the Nimbus-5 played a central role in this program).
2. To initiate satellite studies in the applications areas, particularly the development of advanced sensors for the exploration of natural resources and geophysical phenomena.

The meteorological program called for the application of space technology to increase understanding of the atmosphere and efficiency in making global meteorological observations. The Nimbus-5 provided a versatile orbital platform for a variety of experiments designed to

- Observe atmospheric conditions and processes that influence weather prediction.
- Develop techniques for measuring the global parameters required for modeling atmospheric circulation.

4.5 Data Source

These data are derived from Nimbus-5 ESMR brightness temperatures, originally processed by the Goddard Space Flight Center (GSFC). NSIDC obtained the data from GSFC and reproccesed them to remove coastal and weather contamination, and to include a 15 percent ice threshold.

5 REFERENCES AND RELATED PUBLICATIONS

Comiso, J. C., and H. J. Zwally. 1980. *Corrections for Anomalous Time Dependent Shifts in Brightness Temperature from Nimbus-5 ESMR*. NASA TM-82055. Greenbelt, MD.

Parkinson, C., J. Comiso, H. J. Zwally, D. Cavalieri, P. Gloersen, and W. Campbell. 1987. *Arctic Sea Ice, 1973-1976: Satellite Passive-Microwave Observations.* NASA SP-489.

Parkinson, C., J. Comiso, and H. J. Zwally. 1987. *Satellite-Derived Ice Data Sets No. 2: Arctic Monthly Average Microwave Brightness Temperatures and Sea Ice Concentrations, 1973-1976*. NASA Technical Memorandum 87825.

Pearson, F. 1990. Map Projections: Theory and Applications. CRC Press. Boca Raton, Florida. 372 pages.

Snyder, J. P. 1987. Map Projections - A Working Manual. U.S. Geological Survey Professional Paper 1395. U.S. Government Printing Office. Washington, D.C. 383 pages.

Snyder, J. P. 1982. *Map Projections Used by the U.S. Geological Survey.* U.S. Geological Survey Bulletin 1532.

Wilheit, T. 1972. The Electrically Scanning Microwave Radiometer (ESMR) Experiment. *Nimbus-5 User's Guide*. NASA/Goddard Space Flight Center. p. 59-105.

Zwally, H. J., J. Comiso, C. Parkinson, W. Campbell, F. Carsey, and P. Gloersen. 1983. *Antarctic Sea Ice, 1973-1976: Satellite Passive-Microwave Observations*. NASA SP-459.

Zwally, H. J., J. Comiso, and C. Parkinson. 1981. *Satellite-Derived Ice Data Sets No. 1: Antarctic Monthly Average Microwave Brightness Temperatures and Sea Ice Concentrations 1973-1976*. NASA Technical Memorandum 83812.

6 RELATED DATA COLLECTIONS

Sea Ice Data

7 CONTACTS AND ACKNOWLEDGMENTS

Claire L. Parkinson, Joey C. Comiso, and H. Jay Zwally
NASA Goddard Space Flight Center
Greenbelt, MD, USA 2077

8 DOCUMENT INFORMATION

8.1 Publication Date

August 1999

8.2 Date Last Updated

July 2016

APPENDIX A – EXCTRACTION OF SEA ICE CONCENTRATION FROM ESMR

Within the ice pack, the brightness temperature of a pixel area derives from various sources -- the water and ice within the field of view, and the atmosphere. To a good approximation

$$T_B = C_W \varepsilon_W T_W = C_I \varepsilon_I T_I + T_A$$

where epsilon W, TW, and CW are emissivity, surface physical temperature, and areal percentage of water, and epsilon I, TI and CI are the corresponding values for sea ice. TA is the contribution attributable to the atmosphere and includes the direct upwelling radiation, the downwelling radiation reflected from the surface, and the radiation from space reflected by the surface. Because the reflectance of water is different from that of ice, the atmospheric contribution can be separated into contributions over water, T[AW], and over ice T[AI]. The atmospheric opacity in the polar region has been estimated to be very small and was neglected. Also, C[W] + C[I] = 1 and epsilon [I] was determined empirically to be about 0.92.

The ice concentration, C[I], can thus be determined from equation the above equation:

$$C_I = \frac{T_B - T_0}{\varepsilon_I T_{eff} - T_0}$$

where T[0] = epsilon [W] T [W] + T[AW] is the measured brightness temperature of the water determined from the data, and T[eff] = T[I] + T [AI/epsilong I] is the effective surface physical temperature. The value of T[AW] was calculated by using radiative transfer modeling of the atmosphere (Nieman and Wilheit, private communication) and was estimated over the ocean to be about 8 K. The value of T[AI] is considerably smaller because the reflectivity of ice is substantially lower than that of water, and the contribution of downwelling radiation reflected from the surface is therefore smaller. In the polar regions, the atmospheric contribution to the brightness temperature is minimal because the humidity and the water-vapor content in the atmosphere is very low. Therefore, T[eff] is taken to be equal to T[I]. The appropriate physical temperature, T[I], is the temperature at the top of the sea ice below the snow cover, because most of the observed radiation emanates from a thin top layer of saline ice. in the absence of real-time physical temperature data, T[I] was estimated from a compilation of climatological surface air temperatures (Jenne et al 1974) as follows. The actual temperature of the top sea ice surface lies between the

surface air temperature, T[air], interpolated from the climatological data, and the temperature of the water underneath the ice. It can be expressed by:

$$T_I = T_{air} + f(T_m - T_{air})$$

where T[m] is the melting temperature of ice, and f is an empirical parameter deduced from the ESMR data.